0013-7227/06/$15.00/0
Printed in U.S.A.

Endocrinology 147(7):3375–3390

doi: 10.1210/en.2005-1665

Mining the Mouse Transcriptome of Receptive Endometrium Reveals Distinct Molecular Signatures for the Luminal and Glandular Epithelium

Andrea L. Niklaus and Jeffrey W. Pollard

Departments of Development and Molecular Biology and Obstetrics and Gynecology and Women's Health, Center for the Study of Reproductive Biology and Women's Health, Albert Einstein College of Medicine, Bronx, New York 10461

Epithelia coat most tissues where they sense and respond to the environment and participate in innate immune responses. In the adult mouse uterus, columnar epithelium lines the central lumen and the glands that penetrate the underlying stroma. A nidatory surge of estrogen causes differentiation of the luminal epithelium to the receptive state that permits blastocyst attachment and allows subsequent implantation. Here, using laser-capture microdissection to isolate the luminal and glandular epithelia separately, we have profiled gene expression 2 h before embryo attachment to determine whether there are unique roles for these two epithelial structures in this process. Although most genes were expressed in both compartments, there was greater expression of 153 and 118 genes in the lumen and glands, respectively. In the luminal epithelium, there is enrichment in lipid, metal-ion binding, and carbohydrate-metabolizing enzymes, whereas in the glands, immune response genes are emphasized. *In situ* hybridization to uterine sections obtained from mice during the preimplantation period validated these data and indicated an array of previously undocumented genes expressed with unique patterns in these epithelia. The data show that each epithelial compartment has a distinct molecular signature and that they act differentially and synergistically to permit blastocyst implantation. (*Endocrinology* 147: 3375–3390, 2006)

EPITHELIUM IS A CONSTITUTIVE element of all mammalian tissues and serves a protective function by responding to the environment, participating in innate immunity, and signaling the state of the environment to underlying cellular regions. The diversity of epithelia in the body permits a multitude of organ-specific functions. For example, under the influence of ovarian steroids, the uterine epithelium plays a fundamental role in the establishment and maintenance of pregnancy. Within the endometrium, columnar epithelia line the lumen and glands, respectively. Both are derived from the anterior region of the Müllerian duct.

Across species, the uterine luminal epithelium (LE) is the initial site of embryo attachment, whereas the glandular epithelium (GE) is thought to be the principal source of uterine secretions that are required for the establishment and maintenance of pregnancy (1). The absence of GE and reduced LE in the ovine uterine gland ewe knockout model resulted in a reduced conceptus survival, supporting a fundamental role for GE and their secretions during early pregnancy (2). The precise nature of uterine secretions is not well characterized, but that of LE and GE appear to differ biochemically (3, 4).

There is strong evidence other than differences in biochemical secretions to suggest that under receptive conditions (defined in the mouse as the 24-h period in which the LE will allow attachment of the implanting blastocyst), the LE and GE function as specialized units within the endometrium. The LE has more examples of genes that are solely expressed at periimplantation stages [such as *Areg* (amphiregulin), *Hdc* (histidine decarboxylase), *Irg1* (immunoresponsive gene 1), *Hbegf* (heparin-binding EGF-like growth factor), and *Calb1* (calbindin 28K)] than known in the underlying GE [*Lif* (leukemia inhibitory factor), *Il6st* (IL-6 signal transducer), and *Calca* (calcitonin-related polypeptide-α)] (5, 6). It seems that under receptive conditions, although both epithelial cell types can uniquely express certain genes, many others, also proven to be important for implantation, appear to be coordinately expressed [*e.g. Cdh1* (cadherin 1), *Tro* (trophinin), *Ihh* (Indian hedgehog), *Ptgs1* (prostaglandin-endoperoxide synthase 1 or COX-1)] in both compartments (5, 6). This does not dismiss the importance of genes down-regulated in either or both epithelial cell types during the receptive window such as *Muc1* (mucin 1, transmembrane) (7).

In adult rodents, blastocyst implantation defects arise from the loss of expression of two uterine GE-specific proteins, leukemia-inhibitory factor (8) and calcitonin-related polypeptide-α (9). *WNT7A* expression is restricted to the uterine LE of adult mice (10), and knockout studies show that these mutants are devoid of glands (11) and exhibit an infertile phenotype (12). These mouse models demonstrate the intricate relationship between epithelial cell types that is important for the development of a receptive endometrium. However, the extent of this relationship and the molecular signature that defines them has never been explored largely because of our inability to isolate them.

The use of modern molecular technologies such as cDNA array, laser-capture microdissection (LCM), and improved

First Published Online April 20, 2006

Abbreviations: CT, Cycle threshold; DIG, digoxigenin; E_2, estradiol-17β; GE, glandular epithelium; HPRT, hypoxanthine-guanine phosphoribosyltransferase; LCM, laser-capture microdissection; LE, luminal epithelium; LYZS, lysozyme; P_4, progesterone; QPCR, the established QR-PCR assay; QR-PCR, quantitative real-time RT-PCR, RT, room temperature; SAM, significance analysis of microarrays; SPCR, QR-PCR screen.

***Endocrinology* is published monthly by The Endocrine Society (http://www.endo-society.org), the foremost professional society serving the endocrine community.**

RNA amplification methods has enabled us for the first time to investigate the relationship between LE and GE that is conducive to a receptive environment. The evidence gathered in this study is sufficient to conclude that, at least at the level of transcripts, the LE and GE are specialized epithelial cell compartments. Although these epithelial cell types exhibit cooperative roles during the period of blastocyst implantation, their distinct molecular signatures undoubtedly also play a role in governing the outcome of early pregnancy.

Materials and Methods

Animal and treatments

All animal experiments were conducted under National Institutes of Health guidelines for the care and use of experimental animals. Virgin female CD1 mice 8 wk of age, obtained from Charles River Laboratories, Inc. (Wilmington, MA), were maintained on 12-h light, 12-h dark cycles. Natural pregnancies were followed after detection of the vaginal plug, which was designated as d 1 of pregnancy. To induce and maintain delayed implantation, mice were ovariectomized at noon on d 3 of pregnancy and sc injected daily with progesterone (P_4) from d 3.5–7. At noon on d 7, mice were given a combined dose of P_4 (1 mg) and estradiol-17β (E_2) (10 ng; P_4E_2) to induce uterine receptivity (receptive group). Mice were anesthetized and then killed by cervical dislocation at 8 h after the final injection. All hormones were given sc in peanut oil. Steroid hormones were purchased from Sigma Chemical Co. (St. Louis, MO). Animals of hormone-depleted status (nonreceptive group) were achieved by killing mice 24 h after ovariectomy. Uteri were immediately collected from mice and eight to 10 transverse slices were cut from both horns and placed into a cryomold filled with optimal cutting compound (Tissue-Tek) for immediate freezing on a bed of dry ice.

Laser capture microdissection

Cryosections 8 μm thick of unfixed uterine tissues were placed in 90% ethanol stored within the −20 C cryochamber and fixed for no longer than 2 min. Sections were washed in distilled water, rinsed in absolute ethanol, and counterstained in alcoholic eosin for 10 sec. Rapid washing in absolute ethanol was followed by three subsequent dehydration steps, 2 min each, in absolute ethanol. Within a 60-min time frame of sectioning, approximately five to 15 sections of endometrium were used to initially capture LE cells followed by GE cells using the Arcturus Pix cell II instrument (Arcturus Engineering Inc., Mountain View, CA) as previously described (13).

RNA extraction and cDNA probe preparation

Total RNA was extracted from LCM-captured epithelium using RNeasy Mini Kits (QIAGEN, Valencia, CA) for array and RNeasy Micro Kits (QIAGEN) for quantitative real-time RT-PCR (QR-PCR) according to the manufacturer with amended steps for ethanol precipitation as previously described (13). The yields obtained ranged from approximately 10–150 ng, with the upper range targeted for array analysis. The quality of the RNA was determined using the nano-biosizing assay (Agilent Bioanalyzer; Agilent Technologies, Palo Alto, CA). To remove potential genomic DNA contamination, LCM PCR samples were treated with amplification-grade DNase 1 on a column (QIAGEN) or after resuspension of the pellet (Invitrogen, Carlsbad, CA) for array samples as previously described (13).

The RNA pellet obtained from LCM samples was resuspended into 11 μl of RNase/DNase-free water, and a single round of linear amplification was performed by the *in vitro* transcription T7 promoter method as outlined by the manufacturer's protocol (Ambion's Message Amp TM Kit; Ambion, Austin, TX). Amplified RNA was resuspended into 10 μl RNase/DNase-free water and the yield and quality established by a combination of spectrometry and Agilent Bioanalyzer. Probe cDNA was synthesized from approximately 3.5 μg/μl of amplified RNA and labeled with Cy3 or Cy5 fluorescent dyes (GE and LE, respectively).

Microarrays

Our main goal was to investigate the importance of differential gene expression patterns of LE and GE at periimplantation stages (receptive group). However, array experiments were designed to compare the differential expression of LE *vs.* GE from receptive and nonreceptive groups. This provided further insight as to the likelihood that receptive epithelial gene candidates were hormonally regulated. For each group, LCM samples of LE and GE were collected from one to two animals for hybridization of each array and repeated three to four times.

These samples were simultaneously hybridized to glass 28K cDNA gene chip microarray slides from the Albert Einstein College of Medicine's Array Facility (http://microarray1k.aecom.yu.edu/). Probe preparation and hybridization were performed according to the facility's protocol (http://microarray1k.aecom.yu.edu/) as previously described (14).

After hybridization, the arrays were scanned by Axon Gene Pix 4000A scanner (Axon Instruments, Inc., Foster City, CA). The two fluorescent probes were scanned separately (Cy3 at 532 nm excitation and Cy5 at 635 nm excitation) and the images superimposed using Gene Pix Pro 3.0 software (Axon Instruments). The data were transferred into an MS Excel worksheet and the Cy5/Cy3 ratio for each spot calculated after background subtraction.

Gene expression values were quantified by the two-based log ratio of red channel intensity *vs.* green channel intensity, followed by LOWESS normalization (R-Aroma version 0.85) and MAD scaling to remove the intensity-dependent dye bias and print-tip variation. We restricted our analysis to genes for which the mean fluorescent hybridization signal intensity divided by the median background intensity was at least 1.5.

We used one-class significance analysis of microarrays (SAM, version 1.2), based on Tusher *et al.* (15), to identify differentially expressed genes between LE and GE in the receptive and nonreceptive groups. Comparison of the gene output from one-class analysis of both groups was performed to determine periimplantation-specific genes. SAM assigns a score using a permutation test (based on a modified *t* test) for each gene of a data set. In addition, SAM allows control of the false discovery rate (FDR) by setting a threshold (δ) to the difference between the actual test result and the result from repeated permutations of the tested groups. A *q* value (percent) was assigned to each detectable gene (i) in the array and represents the modified *P* value, measuring the FDR at which a gene is called significant. As the relative difference of each gene (d_i) increases ($d_i > 0$), the *q* value decreases.

To determine gene identity, gene bank accession numbers were used in searches of three independent databases: 1) http://genome-www5.stanford.edu/cgi-bin/source//sourceBatchSearch, 2) http://geneontology.org, and 3) http://microarray1k.aecom.yu.edu. DNA sequencing of all the targets used in PCR and *in situ* validation protocols was performed and revealed more than 95% homology with the published sequences. Using the information gathered from such databases as well as independent research, significant genes in the output from SAM were categorized into common gene function groups for each epithelial cell type.

QR-PCR

To determine the validity of significant gene expression array profiles reported by SAM, quantitative RT-PCR was performed in real time (QR-PCR). To establish the QR-PCR assay, a mass screening of 30 genes was first performed [QR-PCR screen (SPCR)] that included positive and negative controls. The positive control genes known to show preferential expression in the uterine LE or GE under receptive conditions were *Irg1/Calb1* and *Il6st*, respectively. Genes that were shown by array to have similar expression levels in the epithelial cell types such as cathepsin L (*Ctsl*) and cyclin F (*Ccnf*) were used as negative controls (data not shown). LE and GE LCM samples were pooled from receptive uteri of three animals for each cell type. Hence, one sample of cDNA was used to test mRNA expression levels of all genes incorporated in the SPCR (sample size n = 1). The cDNA was made from nonamplified RNA as described.

Several gene targets in the receptive group that showed relatively high SAM scores were selected for additional mRNA analysis using the established QR-PCR assay (QPCR). This differed from the SPCR in that LCM samples were not pooled. LE and GE LCM samples were collected

from receptive uteri of four independent animals for statistical analysis, LE and GE were analyzed as paired samples for each animal (sample size n = 4).

The RNA pellet was resuspended in 10 μl RNase/DNase-free water. First-strand cDNA was reverse transcribed employing a Superscript II RNase kit (90 min at 43 C) (Invitrogen). PCR was performed in real-time using the Prism GeneAmp 5700 (Applied Biosystems, Foster City, CA) to allow amplicon quantification according to the manufacturer's instructions. The 10-μl PCR mixture consisted of 1× SYBR green PCR master mix (Applied Biosystems), cDNA template, forward and reverse primers (ranging from 0.5–1 μM), and 2 μl cDNA. The PCR cycle conditions were one cycle of 50 C for 2 min, one cycle of 95 C for 10 min, and then 40 cycles at 95 C for 15 sec followed by 60 C for 1 min. Primer pairs specific for published cDNA sequences (obtained from http://www.ncbi.nlm.nih.gov/) were designed using Primer3 software (http://frodo.wi.mit.edu/primer3/primer3_code.html). Details of the forward and reverse oligonucleotide primers that were synthesized by Invitrogen appear in Table 1. The mRNA abundances were determined by normalization of the data to the expression levels of 18S rRNA (Universal 18S Primer Pair; Ambion) as well as hypoxanthine-guanine phosphoribosyltransferase (HPRT). In preliminary experiments, serial dilutions of cDNA were analyzed to confirm a linear relationship between cDNA content and quantity of product across the amplification range. As a result, the cDNA was diluted 1:8 for gene of interest and 1:16 for the housekeeping gene. Paired LE and GE samples from all four animals from both experimental groups were analyzed on the same plate and run in triplicate. The omission of cDNA as well as water-only samples served as negative controls. Reaction products were analyzed by dissociation curve profile and by electrophoresis in 2% agarose gel containing 0.5 mg/ml ethidium bromide and visualized over a UV light box.

Relative gene expression of LE *vs.* GE was assessed using the $2^{-\Delta\Delta CT}$ method (16) that calculates 95% confidence intervals. The cycle threshold (CT) indicates the fractional cycle at which the amplified target reaches its threshold. The CT was determined from the exponential phase of the PCR by the SDS 2.2 software. The ΔCT value for a sample is calculated by subtracting the CT of each gene of interest from that of the housekeeping gene. The ΔΔCT of a gene of interest is calculated by subtracting the ΔCT of the GE sample from the ΔCT of the LE sample. An overall ΔΔCT across all of the GE/LE pairs for each gene of interest can then be generated. Thus, $2^{-\Delta\Delta CT}$ represents the fold change in gene expression of the LE over the GE in the receptive endometrial group.

In situ hybridization

Sense and antisense probes were generated from linearized plasmids that contained SP6 or T3 and T7 RNA polymerase sites. The incorporation of digoxigenin (DIG)-labeled nucleotides was performed with the DIG RNA labeling kit (Roche Applied Science, Indianapolis, IN). Uteri were collected and frozen as outlined above from animals at d 1–5 of pregnancy. *In situ* hybridization was performed using 14-μm uterine cryosections mounted on Plus slides (Fisher Scientific, Hampton, NH). PBS (pH 7.4) was used for all washing steps before probe application.

Sections were heated at 50 C for 2 min, air dried, and incubated briefly in chloroform to remove endogenous lipid. After fixation (4% paraformaldehyde, pH 7.4) and acetylation (0.5% acetic anhydride in 0.1 M triethanolamine, pH 8.0, and 0.4% concentrated HCl), each tissue was covered with 100 μl of the hybridization cocktail and a Hybrid plastic coverslip (Sigma) and incubated in a humidified chamber at 58 C for 2 h. The hybridization cocktail consisted of 2× standard saline citrate (SSC) (20× SCC contains 3 M NaCl, 300 mM $Na_3C_6H_5O_7$), 50% formamide, 5× Denhardt's solution (Sigma), and 1 mg/ml salmon sperm DNA (Invitrogen). Incubations in hybridization buffer that contained approximately 0.5 μg/ml of denatured RNA (65 C for 10 min) antisense and sense probes followed for 16 h at 58 C as above.

Slides were washed twice in 2× SSC for 30 min, at 58 C, and then at 37 C. Sections were treated with RNase A (20 μg/ml in 2× SCC; Sigma) at 37 C for 30 min, washed once in 2× SSC for 10 min at 37 C, and washed twice in 0.2× SCC at 58 C for 30 min. After washing with buffer 1 [0.1 M Tris (pH 7.6), and 0.15 M NaCl] for 2 min at room temperature (RT), the slides were incubated in buffer 2 [0.5% blocking reagent (Roche Molecular Biochemicals Co., Indianapolis, IN) in buffer 1] at RT for 10 min. Immunological detection of the hybridized probe was carried out in a humidified chamber with anti-DIG antibody conjugated with alkaline phosphatase (1:5000; polyclonal, Fab fragments from sheep; Roche) diluted in blocking buffer. Slides were washed twice in buffer 1 for 15 min at RT and equilibrated in buffer 3 [0.1 M Tris (pH 9.5), 0.15 M NaCl, 50 mM $MgCl_2$] for 5 min. For color development, slides were incubated overnight at RT in a nitroblue tetrazolium salt/5-bromo-4-chloro-3-indolyl phosphate tablet solution as prepared by the manufacturer (Roche) with levamisole added (200 μg/ml; MP Biomedicals Inc., Levine, CA) to block endogenous alkaline phosphatase activity. The dark purple reaction was stopped with Tris-EDTA solution (0.1 M Tris-HCl, 0.01 M EDTA, pH 8.0). Sections were briefly counterstained with

TABLE 1. Primer pair sequences used for QR-PCR

Gene symbol	Forward	Reverse
Adfp	CCTCAGACTGCTGGACCTTC	AACTGGCTGGTAGGTCCCTT
Arg2	TGATCCAGACAGCCATTTCA	TCTGGCACCTTTCACAACAG
Calb1	ACGGTGGCACACATCTGTAA	TGGATTTGGGGGATATTCAT
Car2	CTGGCCAGCTCTTTCTCATC	CAAGGTTAGCAGCCTCTTGG
Cln5	TAGCAAGCTAACAAAGGCCC	CTCTGGTTTCTCTCCCACCA
Cobl	GGATGGGCATTTATTTGTGG	GTGAGGCAAGAGCTACCAGC
Ctsd	AGTAGAACGTGGTGCCATCC	GGCAGTACTCTGAAGCAGGC
D430044G18Rik	CAGGAATCGTTGGCTCTCTC	TCCAGGGAGACCTTTCCTTT
Eef1g	ACTGCGGTGTAGCATTAGGC	AGAGTGGGACCTCCTTCCAT
Fxyd4	CCAGAGGAGAAGTACGGCAG	CTGGAAAAGCCACTCCACTC
Fyb	CAAAGGTGGCTGGAGCTAAG	GTGCTTAGGGATGGCTTCTG
Gsto1	TTTGTGAGAGGATGCCACAG	GCATTGGAGCTCAGGAGTGT
Hdc	CTGGCCAGCTCTTTCTCATC	CAAGGTTAGCAGCCTCTTGG
IgH(V region) related	GAATGTGACCTGGGGAAAGA	CGGAACATTTCACGGATTCT
Il6st	AGTGAAGGACTGGCTCCTGA	CCCAGGTGTGACTTTGTCCT
Irg1	CCTTGGGTCTTATGCCACAC	GCCAAGAATCCTTCTGCTCA
Lyzs	CTGTGGGATCAATTGCAGTG	TCTCGGTTTTGACAGTGTGC
Nudt4	AACTGGATGGCTTGTCCTTG	ATTCTCCAGTTCCATGTGCC
Ptdsr	ACCTAACCTGGCATCCACTG	TCTCGGGCATGAGGTCTACT
S100g	GCTGGGGAACTCTGACTGAA	TCCTGCAGAAATGAAGAGCA
Slc2a3	GGTGAGGTCCATCAGGTTGT	TCCCTTCTGCCATAGGTCAC
Sprr2a	AGGTAACAGGCAGGCTGAGA	CTGGGGATGCTGAGAATGAT
Srrm1	TTCTTGATCAGAATTCCGGG	CCTCCACAAACTGGTCACCT
Sult1d1	CTGGATGTCTTCAGGAGGGA	CCGGGCTTCAAATGACTCTA
Tm4sf3	ATTCTCCAAGCCACAGCACT	GCTTCTGTCGGACAACACTG
Wfdc2	GCTCAGAATTTGGGTGTGGT	AGGACCAGTGTCAGGTGGAC

0.1% (wt/vol) methyl green, rinsed, and left to air dry before coverslipping.

Results

Microarray

In the one-class analysis of receptive uteri that compared GE *vs.* LE, 271 genes (duplicates omitted) with a FDR of 32 and a predefined δ threshold of 0.41 were differentially expressed at significant levels just before blastocyst implantation. Of these, 153 and 118 had significantly greater expression in the LE and GE, respectively. Figure 1A shows the SAM plot for this comparison.

In the nonreceptive hormone-depleted group, one-class analysis (FDR = 31) showed that 282 genes were differentially expressed in the endometrial epithelial cell types (data not shown). Preferential expression of these genes as in the receptive group was evenly distributed between epithelial compartments with 130 and 152 in LE and GE, respectively (data not shown).

Comparison of LE *vs.* GE differential gene array patterns in both receptive and nonreceptive groups revealed that of 553 candidates, only one gene, *Srrm1*, was duplicated (showing greater expression in GE). Hence, the endometrial LE and GE populations showed diverse molecular signatures during early pregnancy and in mice of depleted hormone status. Therefore, the 270 genes showing differential LE *vs.* GE patterns in the receptive group were a unique gene subset to that of the nonreceptive endometrium and were likely to be regulated by ovarian steroids and related to blastocyst implantation. For this paper, only the genes generated from the receptive group will be the focus of further discussion.

From 271 genes, those of unknown function (these were mostly expressed sequence tags or Riken cDNA clones) were best represented in receptive epithelia (Fig. 1B), comprising at least one quarter of the total number of genes differentially expressed in LE and GE populations (25.5 and 33.1%, respectively). Thus, the remaining 193 genes of known function that ranged in the level of differential expression from approximately 1.5- to 7-fold (Tables 2 and 3) were categorized into groups separately for the 114 genes related to LE (Table 2) and 79 genes related to GE (Table 3). A summary of the percentages of gene function groups represented in LE and GE cell types is shown in Fig. 1B. Because neither gene name nor function could be attributed to epithelial targets in the unknown category, these are not listed in Tables 2 and 3. Genes of functional groups that contained two or fewer members were pooled into a mixed-function group designated as other and comprised 9.8 and 17.8% of the LE and GE populations, respectively. The genes that could be assigned functions in the LE and GE showed great diversity with up to 14 different families represented.

Of the known genes, the most abundant categories (after those of assorted function) represented in both epithelial populations and to equal extents, were enzyme (11%) and cytoskeletal/structural and cell adhesion (9–10%) related genes (Fig. 1B). DNA-binding and transport-associated genes were also found in both LE and GE but to a lesser (<9%) and more varied extent (Fig. 1B). LE had approximately two times as many genes related to DNA binding and half the number of transport-related genes compared with GE (Fig. 1B). Immune-related genes and those involved in signal transduction comprised 7% or less of the total population of genes found in both LE and GE (Fig. 1B).

Unique to the LE population of receptive endometrium in increasing abundance were lipid-, metal ion binding-, carbohydrate-, and protein biosynthesis-related gene families comprising 5.9, 4.6, 4.6, and 2.0%, respectively (Fig. 1B). Conversely, metabolic related genes (4.2%) as well as a small population of mRNA processing genes (2.6%) were only found in GE (Fig. 1B).

Validation by QR-PCR

Validation of mRNA expression of receptive epithelial gene targets was chosen to be performed by PCR in real time owing to the enhanced sensitivity required when using small yields generated from laser-capture samples (17, 18). The QR-PCR assay was established in a preliminary screen (SPCR) using 30 epithelial targets from both LE and GE array lists. SPCR demonstrated that 22 genes correlated 100% with the array data showing significantly greater mRNA expression in LE than GE at periimplantation stages (Fig. 2A). Positive controls used for the SPCR included genes whose expression has been previously shown to be enriched in the LE during the receptive window: *Irg1* (19), *Calb1* (20), and *Hdc* (21).

Included also in the SPCR were eight epithelial targets obtained from the receptive array study that showed significantly greater mRNA expression in the GE than LE compartment and included *Il6st* (22) as a positive implantation-specific control (Fig. 2A).

The 100% correlation of array and SPCR data for 30 implantation-related epithelial candidates, including known positives for specific cell types, demonstrated the accuracy of this assay for determining the reproducibility of differential expression of array gene candidates from laser-captured samples. For the SPCR assay, both 18S rRNA and HPRT were used as reference genes for detecting quantitative mRNA expression in different epithelial cell types. As shown in Fig. 2B, both housekeeping genes produced very similar results for the mean difference in gene expression of 30 candidates with R^2 and slope values of 0.9856 and 0.9589, respectively. Hence there was no significant difference in the mRNA expression in either epithelial cell types as determined by Wilcoxin sign rank test ($P = 0.2948$). Given the low yield of LCM epithelial samples, we used 18S rRNA for future quantitative mRNA assays, because it is more abundant than HPRT.

Expression of selected epithelial targets

A number of genes of interest that also showed higher ranked levels of fold expression in either epithelial cell type were selected for additional analysis. Quantitative mRNA assessment using greater sample numbers was performed using the established QR-PCR assay (QPCR; Fig. 2C). Furthermore, the temporal and spatial expression of novel implantation-related epithelial targets was examined across early pregnant stages using *in situ* hybridization.

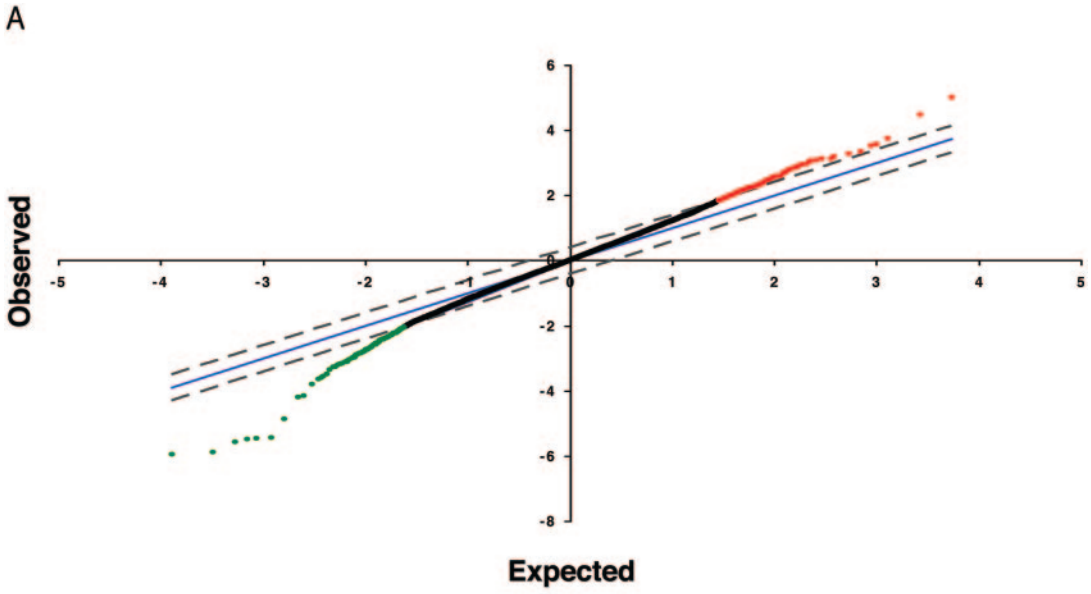

B

Percentage of Genes Represented in Function Groups

Gene Function	LE %	GE %
Carbohydrate Related	4.6	0.0
Cell Cycle	3.9	0.0
Cytoskeletal / Structural & Cell Adhesion	10.4	9.3
Defense Response	5.2	4.2
DNA Binding	9.1	4.2
Enzyme	11.8	11.0
Growth Factors & Signal Transduction	4.6	6.8
Lipid Related	5.9	0.0
Metabolism	0.0	4.2
Metal ion Binding	4.6	0.0
mRNA Processing	0.0	2.6
Other	9.8	17.8
Protein Biosynthesis	2.0	0.0
Transport	2.6	6.8
Uknown	25.5	33.1

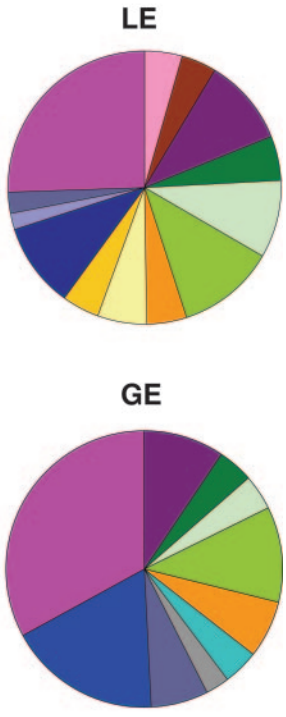

FIG. 1. Differential gene expression in uterine LE and GE. A, SAM scatter plot generated from array analysis of the differential gene expression ($\log_2$) between LE and GE of receptive endometrium. The *solid blue line* shows where the observed relative difference is equal to the expected relative difference. The distance between *dashed lines* is the δ threshold (0.41) that was applied for detection of false positives. The expression of 271 genes/expressed sequence tags (duplicates omitted) was significantly different with a fold change approximately from 1.5- to 10-fold. The *red spots* indicate 153 genes with higher expression in LE, and the *green spots* indicate 118 genes with higher expression in GE. The FDR was 32.1. B, Pie charts showing the relative distribution (percent) of gene function families represented in LE and GE cell compartments of receptive endometrium after SAM analysis of the cDNA array.

Luminal epithelium

Lipid-related genes. The lipid-related fraction of genes enriched in the LE of uteri from the receptive group was of interest to us given the existing knowledge and known progesterone regulation of uterine lipid content (23). More abundant lipid deposition in LE than GE as detected by Oil Red O staining (see supplemental data on The Endocrine Society's Journals Online web site at http://endo.endojournals.

TABLE 2. SAM ouput of genes more significantly expressed in LE than GE

Gene name	Accession no.	Symbol	Fold change
Carbohydrate related			
Glucosaminyl (*N*-acetyl) transferase 2, I-branching enzyme	AW538790	*Gcnt2*	2.27
Phosphomannomutase 1	AU014711	*Pmm1*	1.79
UDP-Gal:βGlcNAc β-1,4-galactosyltransferase, polypeptide 6	AU022389	*B4galt6*	1.78
UDP glucuronosyltransferase 1 family, polypeptide A6A	AW558053	*Ugt1a6a*	1.71
Phosphomannomutase 1	AA387369	*Pmm1*	1.65
Absent in melanoma 1	AA458194	*Aim1*	1.63
Lectin, galactose binding, soluble 3	AA403841	*Lgals3*	1.63
Cell cycle			
B-cell translocation gene 1, antiproliferative	AW546738	*Btg1*	2.37
Replication protein A3	AU017038	*Rpa3*	2.19
Cyclin L1	AU017004	*Ccnl1*	1.67
Cell division cycle 5-like (*S. pombe*)	AU019036	*Cdc5l*	1.59
Retinoblastoma 1	AA427019	*Rb1*	1.55
Cell division cycle associated 4	AU024577	*Cdca4*	1.52
Cytoskeletal/structural and cell adhesion			
Cortactin binding protein 2	AU040881	*Cttnbp2*	4.64
Tetraspanin 8	C76820	*Tspan8*	4.30
Small proline-rich protein 2A	AI414574	*Sprr2a*	4.15
Calponin 3, acidic	C86934	*Cnn3*	3.75
Junction adhesion molecule 2	AU042231	*Jam2*	3.09
Claudin 7	AU015077	*Cldn7*	3.00
Ankyrin 3, epithelial	AI426662	*Ank3*	2.74
TGF-β induced	AA268592	*Tgfbi*	2.40
Integrin α6	AW556992	*Itga6*	2.21
Radixin	AU022468	*Rdx*	2.06
Agrin	AA276537	*Agrn*	2.00
Tropomodulin 3	AA203922	*Tmod3*	1.98
Shroom	AA061732	*Shrm*	1.73
Microtubule-associated protein 4	AW544521	*Mtap4*	1.71
Ras homolog gene family, member Q	AA271510	*Rhoq*	1.71
Protein tyrosine phosphatase, receptor type, F	AW548091	*Ptprf*	1.70
Defense response			
Histocompatibility 2, complement component factor B	W18121	*H2-Bf*	5.22
FYN binding protein	NM_019406	*Fyb*	4.64
Haptoglobin	AU041519	*Hp*	4.25
WAP four-disulfide core domain 2	AA105830	*Wfdc2*	3.94
Histidine decarboxylase	AA118747	*Hdc*	3.48
B-cell linker	C87337	*Blnk*	3.28
Nuclear factor of κ light polypeptide gene enhancer in B-cells inhibitor, ζ	AW545558	*Nfkbiz*	1.84
Tumor-associated calcium signal transducer 2	AI426251	*Tacstd2*	1.67
DNA binding			
Nuclear factor, erythroid derived 2, like 2	AW548328	*Nfe2l2*	2.98
General transcription factor IIIC, polypeptide 4	AU017413	*Gtf3c4*	2.73
Y box protein 1	AU015592	*Ybx1*	2.66
Wiskott-Aldrich syndrome-like (human)	AU045291	*Wasl*	2.05
OVO homolog-like 1 (*Drosophila*)	AW555629	*Ovol1*	2.04
High mobility group nucleosomal binding domain 3	AI449254	*Hmgn3*	1.95
Zinc finger protein 36	AI893411	*Zfp36*	1.94
RIKEN cDNA C230073G13 gene	AA260654	*C230073G13Rik*	1.83
TATA box binding protein	AU019062	*Tbp*	1.80
THAP domain containing 11	AU024242	*Thap11*	1.80
Polybromo 1	AW558386	*Pb1*	1.65
Chromodomain helicase DNA binding protein 1	AW555109	*Chd1*	1.61
Poly (ADP-ribose) polymerase family, member 12	AI448438	*Parp12*	1.61
RIKEN cDNA F830020C16 gene	AA119003	*F830020C16Rik*	1.53
Enzyme			
Glutathione S-transferase ω1	AU040215	*Gsto1*	6.42
Cathepsin D	AW554219	*Ctsd*	4.68
Nudix (nucleoside diphosphate linked moiety X)-type motif 4	AU016024	*Nudt4*	3.84
Nudix (nucleoside diphosphate linked moiety X)-type motif 19	AU016790	*Nudt19*	3.70
Processing of precursor 4, ribonuclease P/MRP family, (*S. cerevisiae*)	AU042817	*Pop4*	3.38
RAB GTPase activating protein 1-like	AA209544	*Rabgap1l*	3.36
ATPase, H^+ transporting, V1 subunit A, isoform 1	AW545297	*Atp6v1a1*	2.67
Protein phosphatase 2, regulatory subunit B, δ-isoform	AA462108	*Ppp2r2d*	2.65
5′-nucleotidase, ecto	AI447772	*Nt5e*	2.59
Choline dehydrogenase	AU041468	*Chdh*	2.56
Protease, serine, 23	AI452270	*Prss23*	2.42
Ubiquitin-specific protease 32	AA260702	*Usp32*	2.31

TABLE 2. *Continued*

Gene name	Accession no.	Symbol	Fold change
Abhydrolase domain containing 3	AU018472	*Abhd3*	2.12
PAK1 interacting protein 1	AW544924	*Pak1ip1*	1.97
Cytochrome B5 reductase 4	AU017987	*Cyb5r4*	1.93
Adenylate kinase 2	C85735	*Ak2*	1.89
Glutamic pyruvate transaminase (alanine aminotransferase) 2	AA080443	*Gpt2*	1.89
Histone deacetylase 1	AA451208	*Hdac1*	1.64
Growth factors and signal transduction			
SH3-binding kinase 1	W67049	*Sbk1*	3.71
Fibroblast growth factor receptor 2	AW556123	*Fgfr2*	2.79
Protein phosphatase 2, regulatory subunit B, δ-isoform	AA462108	*Ppp2r2d*	2.65
Syndecan binding protein	AW537357	*Sdcbp*	2.25
Purinergic receptor P2Y, G-protein coupled, 14	AI448454	*P2ry14*	1.95
Opsin (encephalopsin)	AI450814	*Opn3*	1.60
Bone morphogenetic protein receptor, type 1A	C87663	*Bmpr1a*	1.51
Lipid related			
Immunoresponsive gene 1	AI323667	*Irg1*	5.01
Adipose differentiation related protein	AW555596	*Adfp*	4.32
Ethanolamine kinase 1	BC023950	*Etnk1*	2.84
Sortilin-related receptor, LDLR class A repeats-containing	AW556021	*Sorl1*	2.44
Male sterility domain containing 2	AU017179	*Mlstd2*	2.34
Glycolipid transfer protein	C77053	*Gltp*	2.05
Fatty acid synthase	AW552727	*Fasn*	1.85
Phosphatidylglycerophosphate synthase 1	AA212241	*Pgs1*	1.44
Arachidonate lipoxygenase, epidermal	C88083	*Alox12e*	1.42
Metal ion binding			
Carbonic anhydrase 2	AA122925	*Car2*	5.53
Calbindin-28K	AU041945	*Calb1*	4.69
S100 calcium binding protein G	AU040803	*S100g*	2.74
EF hand domain containing 1	AU019616	*Efhd1*	1.87
ATPase, class VI, type 11A	AU040689	*Atp11a*	1.63
Solute carrier family 25, member 25	AA064156	*Slc25a25*	1.60
ATPase, class VI, type 11A	W18278	*Atp11a*	1.57
Potassium channel tetramerization domain containing 12	AW544440	*Kctd12*	1.50
Protein biosynthesis			
Eukaryotic translation elongation factor 1γ	AW551894	*Eef1g*	3.73
Expressed sequence BF642829	AU043741	*Mrps6*	3.63
Transmembrane, prostate androgen induced RNA	AA144094	*Tmepai*	1.62
Transport			
FXYD domain-containing ion transport regulator 4	AU046167	*Fxyd4*	3.12
ATPase, H^+ transporting, lysosomal V0 subunit A isoform 4	AW558117	*Atp6v0a4*	1.59
Nucleoporin 50	AW556935	*Nup50*	1.49
B-cell receptor-associated protein 29	AW557655	*Bcap29*	1.41
Other			
Ceroid-lipofuscinosis, neuronal 5	AW542388	*Cln5*	4.91
Cordon-bleu	AI413789	*Cobl*	2.95
Teratocarcinoma expressed, serine rich	AW536197	*Tera*	2.55
CCR4 carbon catabolite repression 4-like (*S. cerevisiae*)	AU043840	*Ccrn4l*	2.34
Coxsackievirus and adenovirus receptor	C87757	*Cxadr*	2.23
Squamous cell carcinoma antigen recognized by T cells 2	C86043	*Sart2*	2.15
Nuclear protein 1	AU041522	*Nupr1*	2.08
C1q domain containing 1	AA119641	*C1qdc1*	1.97
F-box protein 11	AI447777	*Fbxo11*	1.88
Fragile X mental retardation gene 1, autosomal homolog	AW558336	*Fxr1 h*	1.77
RAS, dexamethasone-induced 1	AU042021	*Rasd1*	1.68
Cofactor required for Sp1 transcriptional activation, subunit 2	C87652	*Crsp2*	1.53
Breast carcinoma amplified sequence 3	AU018402	*Bcas3*	1.51
Fibronectin type III domain containing 5	AW556555	*Fndc5*	1.49
Dedicator of cytokinesis 9	AI451373	*Dock9*	1.49

org) presented technical difficulties for *in situ* hybridization. Background DIG-alkaline phosphatase staining produced by lipid-enriched epithelial sites was eliminated by chloroform pretreatment before fixation and hybridization steps as described in the supplemental data.

In the lipid-related genes, the mRNA expression of *Etnk1* was significantly elevated by 3-fold in the LE of receptive endometrium. The hybridization pattern for *Etnk1* appeared to be implantation specific (Fig. 3). Hence, there was minimal mRNA expression in the LE on d 2 of pregnancy, which reached peak levels on d 4 of pregnancy and then was reduced after implantation on d 5 (Fig. 3). The decidual cell reaction and GE peripheral to the implantation site on d 5 of pregnancy showed weak expression. The GE had minimal or no *Etnk1* expression across pregnancy (Fig. 3). Uniform and weak hybridization staining in both LE and GE of immature

TABLE 3. SAM ouput of genes more significantly expressed in GE than LE

Gene name	Accession no.	Symbol	Fold change
Cytoskeletal/structural and cell adhesion			
Actin-binding LIM protein 1	AA197466	*Ablim1*	3.82
Decorin	AW556372	*Dcn*	2.44
Growth arrest specific 6	AW557878	*Gas6*	2.38
Integral membrane protein 2C	AU041202	*Itm2c*	2.16
Microfibrillar associated protein 5	AA037995	*Mfap5*	2.05
Enabled homolog (*Drosophila*)	AA444365	*Enah*	2.00
Endothelial cell-specific adhesion molecule	AW543751	*Esam1*	1.84
Cadherin 5	AA435117	*Cdh5*	1.71
RIKEN cDNA D030005H02 gene	AA203798	*D030005H02Rik*	1.60
Dynein, cytoplasmic, intermediate chain 1	AI608513	*Dncic1*	1.59
Moesin	C79581	*Msn*	1.55
Defense response			
Rearranged mRNA for Ig heavy chain (V region)	AA177218	*mRNA IgH*	6.30
Arginase type II	AU043044	*Arg2*	5.70
Lysozyme	C86395	*Lyzs*	4.60
Histocompatibility 2, class II, locus DMa	AU042338	*H2-DMa*	3.26
V-set and Ig domain containing 2	AU040484	*Vsig2*	3.10
DNA binding			
Ring finger protein 141	AU022812	*Rnf141*	2.56
KH-type splicing regulatory protein	C76318	*Khsrp*	2.34
RIKEN cDNA 5730507A11 gene	AW543834	*Nr6a1*	1.91
Zinc finger protein 218	AW556161	*Zfp218*	1.53
RIKEN cDNA A430091O22 gene	AW537758	*A430091O22Rik*	1.50
Enzyme			
Sulfotransferase family 1D, member 1	AA275042	*Sult1d1*	4.08
Mannosidase, βA, lysosomal	AI427701	*Manba*	2.84
3′-Phosphoadenosine 5′-phosphosulfate synthase 1	AW538574	*Papss1*	2.20
Retinol dehydrogenase 10 (all-*trans*)	AU019851	*Rdh10*	2.14
Ubiquitin specific protease 33	AA210309	*Usp33*	2.07
UDP-glucose pyrophosphorylase 2	AW554722	*Ugp2*	2.02
RIKEN cDNA 4833421E05 gene	AU014889	*4833421E05Rik*	1.98
Carboxylesterase 3	AU042959	*Ces3*	1.96
ADP-ribosylhydrolase like 2	AU017617	*Adprhl2*	1.91
Myoinositol 1-phosphate synthase A1	AW555806	*Isyna1*	1.87
Dihydrouridine synthase 2-like (SMM1, S. cerevisiae)	AW544232	*Dus2l*	1.87
Tissue inhibitor of metalloproteinase 2	AW557582	*Timp2*	1.85
Insulin-degrading enzyme	AA111232	*Ide*	1.55
Growth factors and signal transduction			
IL-6 signal transducer	AU016341	*Il6st*	2.83
Phosphatidylserine receptor	AW557684	*Ptdsr*	2.62
Twisted gastrulation homolog 1 (*Drosophila*)	C85287	*Twsg1*	1.92
GH receptor	AW547026	*Ghr*	1.83
Adenylate cyclase activating polypeptide 1 receptor 1	AW547403	*Adcyap1r1*	1.69
RIKEN cDNA 4930448O17 gene	AW554244	*4930448O17Rik*	1.53
Stress 70 protein chaperone, microsome-associated, human homolog	AA265364	*Stch*	1.52
SCY1-like 1 (*S. cerevisiae*)	AU016501	*Scyl1*	1.50
Metabolism			
Gulonolactone (L-) oxidase	BC028828	*Gulo*	5.63
Cystathionase (cystathionine γ-lyase)	AU044849	*Cth*	4.28
Solute carrier family 23 (nucleobase transporters), member 2	AW546130	*Slc23a2*	3.11
Liver glycogen phosphorylase	AW550027	*Pygl*	2.39
Cystathionine β-synthase	AU020595	*Cbs*	2.22
mRNA processing			
Serine*/arginine repetitive matrix 1 (*overlap nonreceptive gp)	AI322433	*Srrm1*	4.70
RNA-binding motif protein 16	AW549693	*Rbm16*	2.85
Endoplasmic reticulum (ER) to nucleus signaling 1	AW555403	*Ern1*	1.63
Transport			
Solute carrier family 2 (facilitated glucose transporter), member 3	C79519	*Slc2a3*	3.99
RIKEN cDNA E130014H10 gene	AU016965	*E130014H10Rik*	3.24
Transmembrane and coiled-coil domains 3	C87304	*Tmco3*	2.55
Serum/glucocorticoid regulated kinase	AU042681	*Sgk*	2.48
Vacuolar protein sorting 41 (yeast)	AU040750	*Vps41*	2.31
Mannose-6-phosphate receptor, cation dependent	AU017465	*M6pr*	2.19
Sec61 β-subunit	AI326121	*Sec61b*	1.71
Blocked early in transport 1 homolog (*S. cerevisiae*)	AW555236	*Bet1*	1.63
Other			
Synaptotagmin-like 4	AU016846	*Sytl4*	3.96
Formin-binding protein 1	C76662	*Fnbp1*	3.44

TABLE 3. *Continued*

Gene name	Accession no.	Symbol	Fold change
SH3 domain and tetratricopeptide repeats 2	AW552849	*Sh3tc2*	3.38
Fibronectin type III domain containing 3B	C85576	*Fndc3b*	3.22
Peptidylglycine α-amidating monooxygenase	AI323455	*Pam*	2.94
Aldo-keto reductase family 1, member C19	AW551736	*Akr1c19*	2.80
WW domain binding protein 5	AW551726	*Wbp5*	2.50
Immediate early response 3	AI323680	*Ier3*	2.11
DNA segment, Chr 12, ERATO Doi 647, expressed	W99140	*D12Ertd647e*	2.10
DNA cross-link repair 1A, PSO2 homolog (*S. cerevisiae*)	AU022226	*Dclre1a*	2.08
BTB (POZ) domain containing 15	AU024758	*Btbd15*	1.84
Purinergic receptor P2Y, G-protein coupled, 14	AU044581	*P2ry14*	1.81
Von Hippel-Lindau syndrome homolog	AW548526	*Vhlh*	1.77
Similar to kinesin-like protein	AU045482		1.75
F-box and WD-40 domain protein 5	AW555560	*Fbxw5*	1.74
WW domain binding protein 5	AI414288	*Wbp5*	1.72
Transcription elongation factor A (SII)-like 8	AA038416	*Tceal8*	1.70
Protein (peptidyl-prolyl *cis/trans* isomerase) NIMA-interacting 1	AW544350	*Pin1*	1.67
Zinc finger, C^3HC type 1	AW549666	*Zc3hc1*	1.60
G protein-coupled receptor-associated sorting protein 1	AW553322	*Gprasp1*	1.57
Similar to ATP-dependent chromatin remodeling protein SNF2H	AA415240		1.50

(4 and 6 wk) and nonpregnant uteri (data not shown) confirmed that *Etnk1* is maximally expressed in the LE compartment during the implantation window. The preferential expression of *Etnk1* in the LE rather than GE just before implantation was confirmed by QR-PCR as shown in Fig. 2C.

Adfp was an example of another lipid-related gene whose 4-fold more abundant expression in LE than GE of receptive endometrium was confirmed by QR-PCR (Fig. 2A).

Cytoskeletal/structural and cell adhesion. Under receptive conditions, *Sprr2a* and *Tspan8*, were among the top bracket of cytoskeletal/structural and cell adhesion-related genes with the greatest levels of expression in the LE than GE. The greater than 4-fold mRNA expression in the LE than GE as shown by array just before blastocyst attachment was supported by QR-PCR findings for both genes (Fig. 2, A and C). Although there was greater mRNA expression of *Sprr2a* in LE than GE on d 4 of pregnancy as shown by QR-PCR (Fig. 2, A and C) and *in situ* hybridization findings, the expression was weak compared with the intense staining seen on d 1 of pregnancy (data not shown). Many other whole-uteri array mouse studies have also found that this gene, a structural component of the epidermal cornified cell envelope, is estrogen regulated (24–26), is primarily located in epithelia, and is implantation specific (27).

Defense responses. Fyb, *Wfdc2*, and *Hdc* were among the immune-related genes whose expression was significantly upregulated under receptive conditions by at least 3.5-fold more in the LE than GE. QR-PCR confirmed that all three genes were indeed preferentially expressed in the LE surface of P_4E_2-injected endometria of delayed mice (Fig. 2, A and C).

In the uterus, *Hdc* is a major source of histamine, released from mast cells of the uterine stroma (28), and is also capable of inducing an edematous response (29). *Hdc* expression has been shown previously to be more abundant in the LE on d 4–5 of pregnancy in the mouse (21). Thus, this gene serves as a good positive control for our data set as shown by QR-PCR (Fig. 2A).

Fyb, also known as SLP-76-associated protein of 130 kDa (SLAP-130) or adhesion and degranulation-promoting adapter protein (ADAP), is thought to be exclusively expressed in mononuclear cells of the hematopoietic lineage with preferential expression in T lymphocytes and monocytes (30). We confirmed by hybridization the preferential mRNA expression of *Fyb* in immune cells of the stroma, immediately underlying the basement membrane of the LE on d 4 of pregnancy (data not shown). These *Fyb*-positive immune cells, given their location, were obviously cocaptured with LE at the time of sample collection.

LE expression of the natural antimicrobial named *Wfdc2* was maximal on d 3 of pregnancy, weakened slightly on d 4, and was further reduced on d 5 with isolated staining in the decidualized region of the endometrium as shown by *in situ* hybridization (Fig. 4A).

Other than its biological function of capturing free hemoglobin, haptoglobin (HP) has also been suspected to play an important role in inflammation (31). Although weak in expression throughout the endometrium on d 2 of pregnancy, a robust increase of *Hp* mRNA only in the LE compartment was noted on d 3–4 of pregnancy with moderate staining of the decidual reaction on d 5 also (data not shown).

Enzyme. Of all the genes significantly expressed by the array, *Gsto1* and *Cstd*, members of the enzyme-related gene fraction, showed the greatest increase in mRNA expression (5- to 7-fold) in the LE rather than GE just before implantation. QR-PCR analysis of LE and GE isolated by LCM 8 h after P_4E_2 injection of delayed-implantation mice supported the preferential expression of these genes in the LE compartment (Fig. 2, A and C) as well as others such as *Nudt4* (Fig. 2A).

The sudden and dramatic appearance of *Gsto1* mRNA expression in LE on d 3–4 of pregnancy (Fig. 4B) with an absence of staining by d 5 as shown by *in situ* hybridization confirmed that this gene was specific to the implantation window in mice. Not previously described in the endometrium, *Gsto1* is an unusual isoform of a member of the glutathione S transferase (GST) family, which functions as an antioxidant. The GE showed complete absence of expression for *Gsto1* at all stages of pregnancy examined (Fig. 4B).

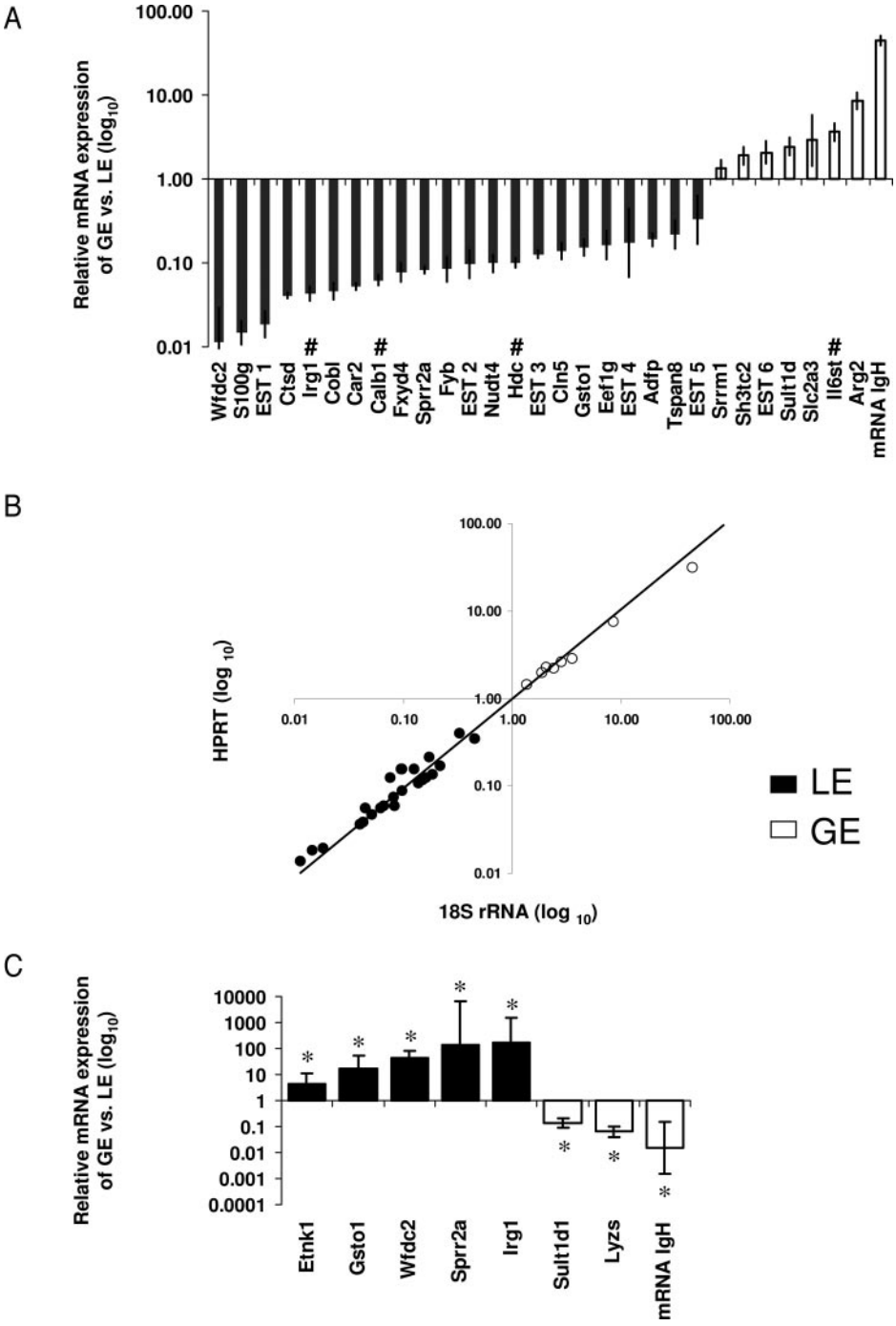

FIG. 2. Validation of DNA microarray data by QR-PCR. A, The mean fold difference (±SEM generated from triplicates) of mRNA expression (relative to 18S rRNA) of different gene targets in GE compared with LE of receptive endometrium. Initially, a QR-PCR screen (SPCR) using pooled LCM samples from three animals per epithelial cell type (n = 1) was used to determine the accuracy of array gene targets that showed significant differential expression during the period of uterine receptivity. The 95% confidence intervals that do not cross 1 are considered significant. More abundant gene expression in either LE or GE components is designated by the *black* and *white bars*, respectively. #, Control genes. B, The correlation between the mean difference in target gene mRNA expression of epithelial cell types using both HPRT mRNA and 18S rRNA as reference genes ($\log_{10}$ scale). The *solid line* shows the line of best fit from a linear regression plot (R^2, 0.9856; slope, 0.9589), showing that there was a great similarity between the data generated from the two reference genes. Each target gene from the data set in this figure is represented as a *circle*, with more abundant expression in LE or GE components denoted by the *black* and *white circles*, respectively. C, The mean fold difference (±SEM) of mRNA expression (relative to 18S rRNA) of various gene targets in GE compared with LE of receptive endometrium. A larger sample size (n = 4) was used in established QR-PCR assays to further investigate the differential mRNA expression of genes of interest in one epithelial cell type or the other (QPCR). *, The 95% confidence intervals that do not cross 1 are considered significant. The significantly more abundant mRNA expression in LE and GE is denoted by *black* and *white bars*, respectively.

Growth factor and signal transduction. In the category of growth factor and signal transduction, *Sbk1* showed 3- to 4-fold significantly greater expression in the LE than GE just before implantation. Hybridization staining showed that on d 2 of pregnancy, the level of *Sbk1* expression was similar in LE and GE but that there was a robust increase in the LE surface expression on d 3–4 with a sharp decline on d 5 of pregnancy (data not shown).

Other groups. Under receptive conditions, calcium- and zinc-binding-related genes, *Calb1/S100g* and *Car2*, respectively, were elevated approximately three to six times higher in the LE than GE. The robust increase in and preferential mRNA expression of these genes in LE was confirmed by QR-PCR (Fig. 2A). Calbindin 28K is a well-established epithelial marker of endometrial receptivity in mice and primates (20).

Cob1 has recently been identified as an important gene in axial patterning (32). Its mRNA expression was confirmed to be significantly more expressed in LE than GE by QR-PCR (Fig. 2A) as well as in tissue sections on d 4–5 of pregnancy (data not shown). In addition, *Cln5*, a lysosomal-related gene, was found to have preferential expression in LE during the implantation window (data not shown), which was also sup-

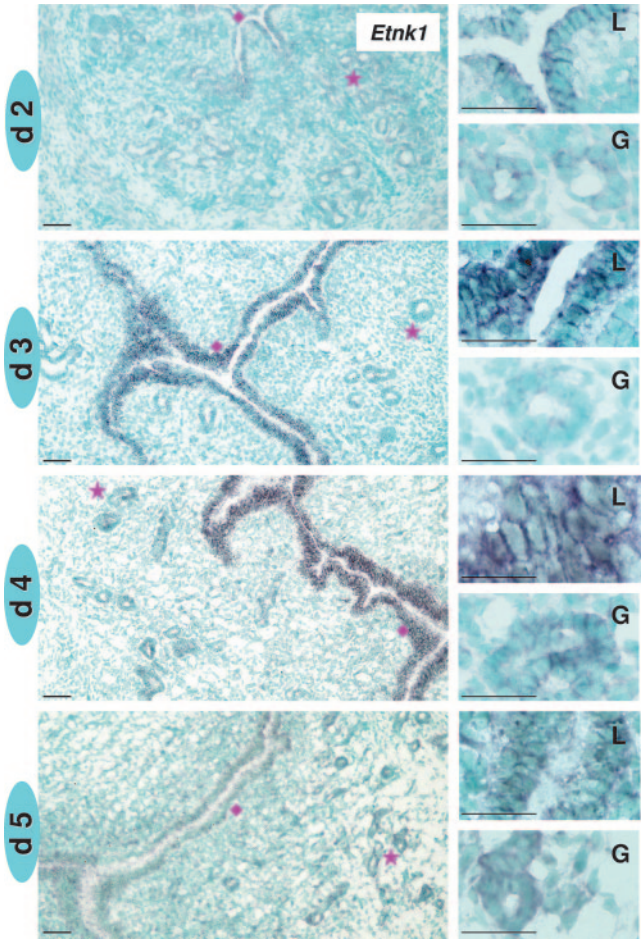

FIG. 3. *Etnk1* is preferentially expressed in LE before implantation, as shown by the *in situ* hybridization pattern of *Etnk1* in frozen transverse sections of uteri from d 2–5 of pregnancy. Each stage of pregnancy shown in the *ovals* on the *left* has two *insets* from LE (L) and GE (G) regions as denoted by a *pink diamond* and *star*, respectively, showing higher-magnification views of differential staining. Sections are counterstained with methyl green. *Scale bars*, 40 μm. The mRNA expression of *Etnk1* was not apparent in the endometrium until d 3 of pregnancy where it was primarily found in LE. By d 4 of pregnancy, LE-specific *Etnk1* expression had peaked but was diminished by d 5 of pregnancy.

ported by QR-PCR findings (Fig. 2A). *Eef1g*, involved in protein biosynthesis, was determined to be 4-fold preferentially expressed in LE of endometrium from P_4E_2-induced delayed-implantation mice as confirmed by QR-PCR (Fig. 2A).

Of the genes of mixed transport function, *Fxyd4* had three times the level of expression in the LE than GE at periimplantation as supported by QR-PCR (Fig. 2A). LE and GE mRNA expression of *Fxyd4* was minimal on d 2 of pregnancy but was significantly elevated in LE on d 3–4 with decreased expression on d 5 of pregnancy (data not shown). FXYD4, also known as corticosteroid hormone-induced factor (CHIF), belongs to the FXYD family of single-membrane-span proteins that have been shown to interact with NaK-ATP and have a general ion transport function (33). Despite having an expression pattern specific to the implantation window, *Chif* null mice are fertile (34).

Glandular epithelia

Defense response. Rearranged mRNA from the Ig heavy chain (V region; mRNA IgH) and *Lyzs* were the most prevalent immune-related genes expressed up to 6-fold higher in isolated GE than LE populations obtained from receptive endometrium. The more abundant expression of these two genes in GE at periimplantation was confirmed by QR-PCR (Fig. 2, A and C) and *in situ* hybridization (only *Lyzs* shown in Fig. 5). The spatiotemporal mRNA expression pattern of *Lyzs* across pregnancy was particularly striking (Fig. 5). Weak staining of GE and underlying stroma was seen on d 2 of pregnancy. By d 3, there was punctate expression of *Lyzs* mRNA in individual cells of GE as well as in stromal cells underlying LE (Fig. 5). Late on d 4 of pregnancy, only punctuate staining of GE remained, which by d 5 was reduced in expression with weak but uniform staining of the decidual zone also (Fig. 5).

The rearranged mRNA Ig heavy chain clone (mRNA IgH) was predominantly expressed in isolated stromal cells throughout pregnancy, which became increasingly abundant and were located within closer proximity of GE as blastocyst implantation approached (not shown). By d 4 of pregnancy, mRNA staining of isolated immune cells cusped the basement membrane of GE in a pattern similar to that of plasma cells, which have been shown to be enriched in endometrium at this time (35). Thus these peri- and intraluminal B lymphocytes were captured in the GE fraction.

In addition, *Arg2* mRNA was found to have 6-fold greater expression in LE than GE by array as supported by QR-PCR (Fig. 2A). *Arg2* encodes an enzyme that has been recently assigned an immune-related role (36) that facilitates periimplantation events.

Enzyme. With 4-fold greater expression in GE than LE of receptive endometrium, which was also supported by QR-PCR (Fig. 2, A and C), *Sult1d1* stood out among the varied list of enzyme-related genes as a potential marker for implantation. Its differential expression pattern was one of the few examples of genes we studied that was significant only when delayed mice were treated with the combination of P_4E_2 and not P_4 alone (data not shown). Indeed, its weak expression on d 2 of pregnancy but marked expression on d 3–4 characterized it as one of few known gland-specific markers of implantation (Fig. 6A). LE showed consistently weak *Sult1d1* expression across pregnancy until d 5 when peripheral GE and decidual cells were also moderately stained (Fig. 6A).

Metabolism. Related to ascorbic acid metabolism, *Gulo* was one of the most abundantly expressed genes preferentially expressed up to 6-fold more in GE of receptive endometrium. *In situ* hybridization confirmed that there was weak LE but intense GE mRNA expression of uteri late on d 4 of pregnancy (Fig. 6B). However, differential epithelial expression patterns were apparent only on d 4–5 of pregnancy as uniform, moderate staining was seen during earlier stages of pregnancy.

Other. Of varying function, *Slc23a2*, *Sh3tc2*, and *Fnbp1* are examples of other genes that showed 3- to 4-fold greater

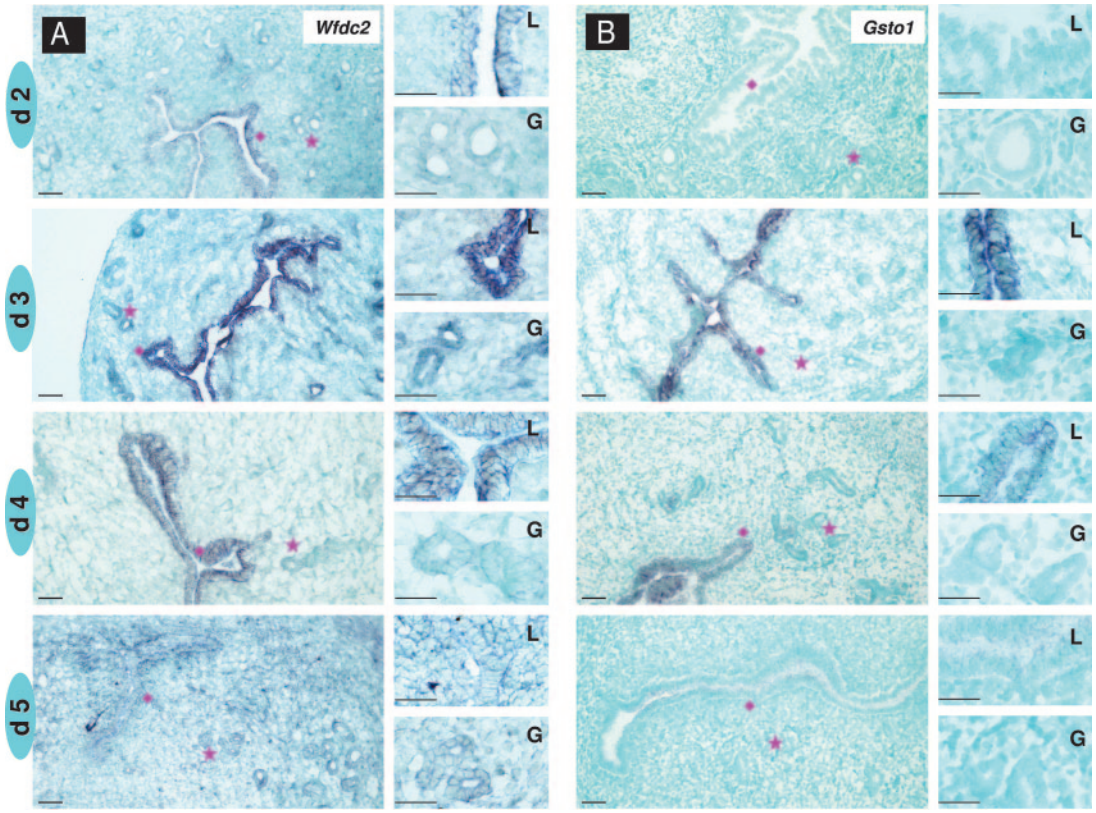

FIG. 4. LE enhanced expression of *Wfdc2* and *Gsto1*, as shown by the *in situ* hybridization staining pattern of *Wfdc2* (A) and *Gsto1* (B) in frozen transverse sections of uteri from d 2–5 of pregnancy. Designations are as in Fig 3. *Scale bars*, 40 μm. A, On d 3 of pregnancy, there was maximal *Wfdc2* mRNA expression of LE with no expression in any other endometrial compartment. As blastocyst implantation approached on d 4 of pregnancy, the preferential staining of LE persisted but was weaker and had almost diminished by d 5. B, The mRNA expression of *Gsto1* was specific to the implantation window, localized only to LE on d 3–4 of pregnancy.

expression in GE than LE at periimplantation stages. QR-PCR confirmed the preferential GE expression of the first two of these genes (Fig. 2A) as did tissue-specific hybridization staining patterns for *D430044G18Rik* and *Fnbp1* on d 4–5 of pregnancy (data not shown).

Discussion

We used LCM to separate RNA samples from uterine LE and GE for cDNA microarray analysis of differential gene expression under receptive and nonreceptive conditions. Using this technology, we have identified numerous genes, such as *Cln5*, *Etkn-1*, *Gsto1*, and *Sult1D1*, whose expression in epithelia is implantation specific and to the best of our knowledge have not been described in this location in the adult mouse. In addition, analysis of the mouse transcriptome and extensive validation by QR-PCR and *in situ* hybridization confirmed that LE and GE exhibit distinct molecular signatures during the period of receptivity in the mouse. Such molecular phenotypes include the representation of unique gene function families such as lipid-, carbohydrate-, and metal-ion-binding-related genes in LE. However, under receptive conditions, expression of many gene families were also represented in both epithelial populations, especially those related to enzymatic and structural functions, that were not found in the nonreceptive conditions. Hence, the dynamic relationship between LE and GE to induce uterine receptivity is specialized but also synergistic.

Although we have largely focused on implantation, our array analysis also revealed that LE and GE have distinct molecular signatures irrespective of the uterine hormone milieu. The 282 genes that showed differential expression under hormone-depleted status (nonreceptive group) were not further investigated in this paper, but the result itself suggests that the molecular relationship between endometrial epithelial subtypes is important not just at periimplantation stages but across the mouse reproductive cycle.

Whether cDNA or oligonucleotide derived, all of the arrays performed to date in the adult mouse have used whole uterine samples in an attempt to find ovarian steroid hormone-regulated targets (25–27, 37–40). Hence, our array study is unique in that we have focused on individual endometrial epithelial cell types to evaluate the extent of their relationship in inducing receptive uterine conditions. Given the huge variation in experimental design and data analysis of previous uterine array studies, it is difficult to cross-compare the results to find repeated patterns of true molecular markers of uterine responsiveness. Indeed, the implantation-specific expression patterns of certain epithelial cell types of a receptive endometrium may be diluted by the use of mixed-cell populations. For example, *Wfdc2* (38) was a gene candi-

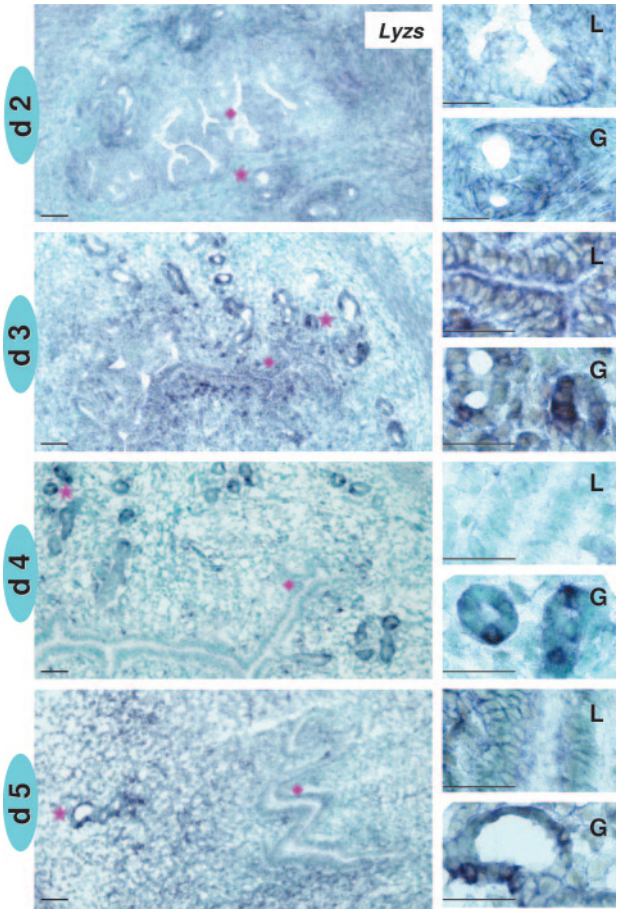

FIG. 5. Expression of *Lyzs* in GE through the preimplantation period. The *in situ* hybridization staining pattern of *Lyzs* in frozen sections of transverse uteri from d 2–5 of pregnancy. Designations are as in Fig. 3. *Lyzs* mRNA expression was not apparent until d 3 of pregnancy where it was expressed in individual immune-related stromal cells underlying LE as well as in isolated cells of most GE. The punctate staining of GE persisted by d 4 with little stromal *Lyzs* mRNA expression. However, by d 5, there was weak decidual cell reaction and some residual glands remained positive.

date found to be decreased in whole uteri from ovariectomized P_4-treated mice. However, by *in situ* hybridization, we found its expression to peak on d 3–4 of pregnancy in the LE.

There is a consistency, however, in the published array data that suggests that less than 6% of all the mouse transcriptome (usually from 1.5–6%) represented on any given chip are regulated by ovarian steroids in the uterus. This is uniform across the many types of targets sought, whether estrogen (26, 37), progesterone (27, 38), or implantation specific (27, 39). This is also the scenario in the literature of human uterine array studies, except endometrial (not whole uterine) samples have been used, where once again, roughly 1–6% of the genome tested seem to be hormonally regulated (41–44).

In this study, we reported that of 19,202 sequences expressed in the uterus of receptive groups, approximately 1.5% showed a significant level of differential expression. This is notable, given that other mouse (27) and human (42, 44) array studies of mixed-cell populations using whole endometrium or uteri taken from the receptive period have reported less than 2.5% hormonal gene regulation of the genome tested. The fact that we found 1.5% from hybridization of only two epithelial cell types is a testament to the diverse molecular nature of the LE and GE of a receptive uterus.

There is some degree of variation in the timing of implantation with natural matings. We used the delayed-implantation mouse model to induce uterine receptivity because this enabled us to control the timing, so that we could examine the endometrium during a defined 2- to 4-h preblastocyst attachment period. We found that the majority of genes examined were expressed in both GE and LE. However, significant differences in the molecular phenotype between epithelial subtypes were found, and this may be key to understanding uterine infertility and disease.

Under receptive conditions, we found more examples of genes solely expressed in the LE than GE. Furthermore, our cDNA array slides were not printed with *Calca*, and the *Lif* cDNA clone consisted of a hybrid sequence (our unpublished data), which made validation of GE-specific targets of receptivity difficult. However, other differentially expressed epithelial markers of uterine receptivity were found. For example, the significantly greater abundance of *Ilst6* (22) mRNA in GE as well as the preferential LE expression of *Hdc* (21) and *Calb1* (20) together with other implantation-specific genes, *Ihh* (45) and *Tro* (46), in both compartments were findings that supported the use of the delayed model to obtain receptive endometrium and validated the novel gene expression patterns that we have described.

In each epithelial cell type, there were distinct gene expression signatures. The increased presence of lipid bodies within the endometrial epithelium during early pregnancy has long been established (47, 48). These are spherical organelles composed of a core of neutral lipids such as triacylglycerols and cholesterol esters that often contain specific populations of proteins bound to their surface (49) like adipose differentiation-related protein. This is the first report of *Adfp* mRNA within the endometrium where we found it more abundantly expressed on the uterine LE surface than in GE at implantation. The exact biological function of adipose differentiation-related protein has not been determined but is believed to be in the intracellular mobilization and storage of neutral lipids (50).

There are also other lipid-metabolizing enzymes such as *Etnk1* that are specifically expressed in the LE compartment. *Etnk1* (ATP:ethanolamine *O*-phosphotransferase, EC 2.7.1.82) is the first enzyme in the CDP ethanolamine pathway, which is primarily important for the biosynthesis of phosphatidylethanolamine, an abundant phospholipid in eukaryotic cell membranes (51). *Etnk1* activities in rodents were isolated from liver many years ago (52), but little is known regarding its expression in the adult mouse. The induction of *Etnk1* primarily in LE during the implantation window could be associated with increased phosphatidylethanolamine synthesis. Overexpression of *Drosophila Etnk1* in a NIH 3T3 cell line (53) protected these cells from apoptotic cell death. Peak levels of *Etnk1* in LE on d 4 followed by a demise in expression on d 5 of pregnancy, is consistent with pre- and postapoptotic cell events in this cell type that allow the implanting embryo to invade. It is proposed that the effects of phosphorylated ethanolamines on cell survival may be mediated by alterations in the composition of the

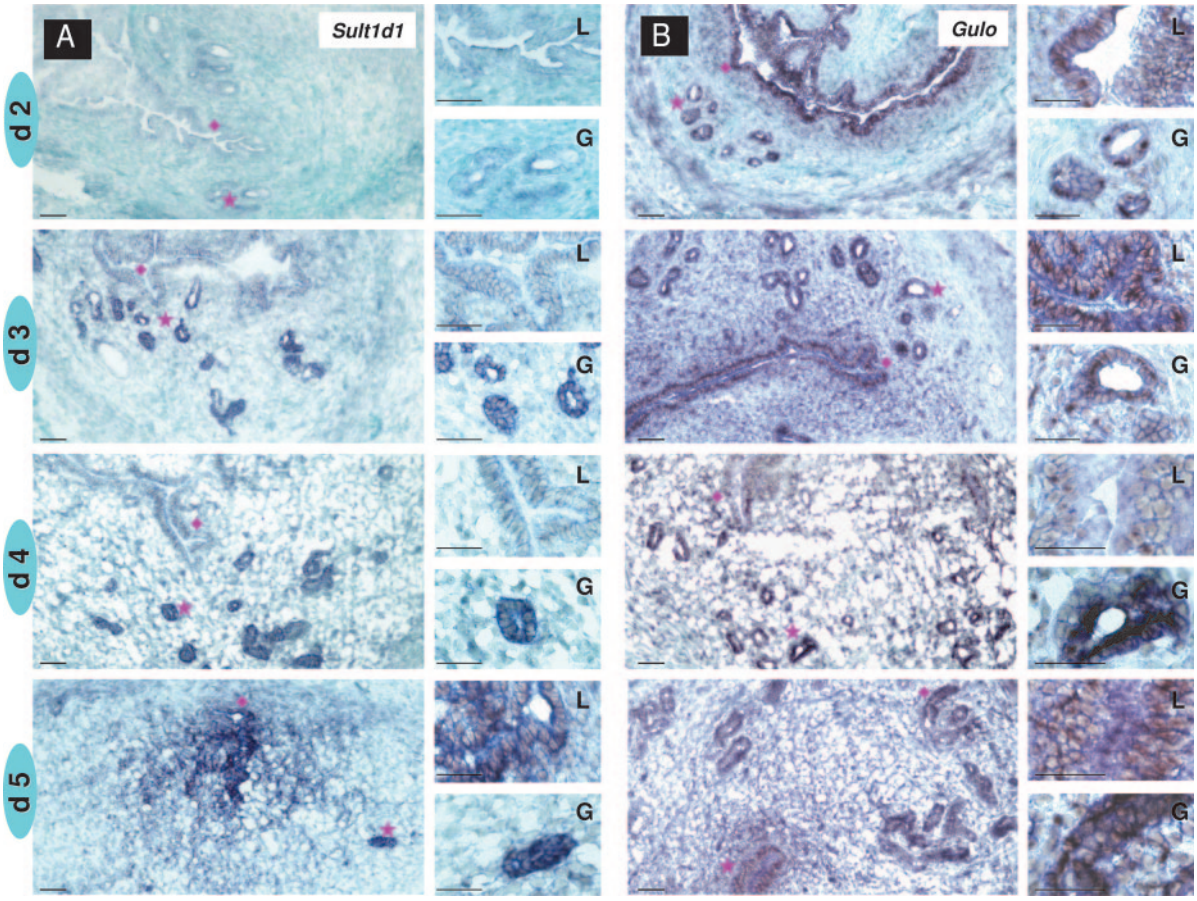

FIG. 6. *Sult1d1* and *Gulo* are preferentially expressed in GE, as shown by the *in situ* hybridization of *Sult1d1* (A) and *Gulo* (B) in frozen sections of uteri from d 2–5 of pregnancy. Designations are as in Fig. 4. *Scale bars*, 40 μm. A, *Sult1d1* mRNA expression was maximal in GE on d 3–4 of pregnancy with negative to weak staining in LE. However, after implantation on late d 5 of pregnancy, Sult1d1 had increased expression in LE and associated decidual cell reaction together with remaining glands. B, *Gulo* mRNA was uniformly expressed in both LE and GE on d 2–3 of pregnancy. However, as blastocyst implantation approached on late d 4 of pregnancy, there was more abundant expression in GE than LE, which was maintained on d 5 of pregnancy.

phospholipids membrane or by a direct block of a key apoptotic enzyme (54).

Another gene that appears to be involved in lipid metabolism is *Irg1*, which has already been shown to be highly up-regulated by P_4 in the LE compartment at the implantation window (19, 55), a result confirmed in this study. There are other genes not found to be differentially expressed in our experiments that appear to play essential functions at implantation, such as the lipooxygenases that convert arachidonic acid to leukotriene A4 (55). The important role that lipid mediators such as prostaglandins and endocannabinoids are thought to be play in the molecular dialogue between embryonic and endometrial surfaces at implantation has been recently emphasized (56).

This study, together with others in both mouse and human uteri, has revealed a large number of immunologically relevant proteins expressed by the uterine epithelium. Previously, we have shown that two epithelial abundant cytokines, colony-stimulating factor 1 (57) and chemokine (C-C motif) ligand 26-like or eotaxin (*CCL11*) (58), are hormonally regulated in the endometrium where they effect macrophage recruitment. Indeed, the uterine epithelium seems to be a rich source of hematopoietic cytokines and growth factors throughout pregnancy, including the implantation phase (59–61). These factors are likely to regulate the innate immune responses to pathogen challenges that may occur during mating, and they may also be involved in wounding responses to the invading blastocyst.

In addition to these growth factors, there are also many proteins that play a role in mucosal immunity through their bactericidal functions (62). Among these, the whey acidic protein (WAP) motif protein, WAP four-disulfide core domain 2, identified in the current study together with other natural antimicrobial peptides, such as β-defensins and secretory leuckocyte protease inhibitor (SLPI), are thought to be key mediators of the innate immune defense critical for successful implantation and pregnancy. The WAP domains are usually small secretory proteins that exhibit a variety of functions, including those that affect growth and differentiation (63). In fact, they are the major whey proteins in mouse milk (64). Little is known about the expression pattern and function of WAP four-disulfide core domain 2 in rodents, especially in reproduction. However, in recent array studies of primate endometrium, the expression of *Wfdc2* was significantly up-regulated during the secretory phase of women (65) and monkeys (66), which coincided with the

period of receptivity. Although Yanaihara *et al.* (65) localized peak expression of *Wfdc2* to the epithelium, they did not distinguish between subepithelial populations. Whole-uterine array studies mining for P_4-regulated genes in mice (38) failed to identify this gene as we have in isolated LE samples of receptive endometrium.

Lysozyme (LYZS), a bacteriolytic enzyme also known as muramidase, is typically expressed in hematopoietic cells of the macrophage and granulocyte lineage. In mammals, LYZS is also an important component of innate immunity against common pathogens at mucosal surfaces where it is confined to specialized epithelial cells including the serous (but not mucinous) glands (67) and Paneth cells (68) of the respiratory and gastrointestinal tract (terminal ileum), respectively. Although uterine *Lyzs* expression has been shown to vary across the mouse reproductive cycle (26), this is the first report to demonstrate epithelial-specific mRNA expression during the receptive window. The punctuate staining of select GE cells at periimplantation stages described here was striking and similar to LYZS protein expression of gut epithelium described in human patients with ulcerative colitis and Crohn's disease (69). Changes in the cyclic and early pregnancy expression of endometrial *Lyzs* likely parallels the changing populations of macrophages with varying hormonal milieu (57).

The preferential expression of cytoskeletal and structural genes such as *Sprr2a* and *Tspan8* on the LE surface at periimplantation stages highlights the specialized molecular phenotype that this structure adopts to induce receptivity. Associated with barrier function for protection against water loss (70) and infection (71), the down-regulated LE expression of *Sprr2a* mRNA leading up to d 5 of pregnancy in mice likely facilitates blastocyst implantation.

In the present study, we found *Sult1d1* to be almost exclusively expressed in the uterine GE during the implantation period of mice. This enzyme belongs to a family of cytosolic sulfotransferases that mediate sulfation and play a critical role in the homeostasis, regulation, and detoxification of biologically active endogenous and environmental chemicals (72). Northern blot analysis of a wide spectrum of different tissues revealed that cDNA expression of the original mouse *Sult1d1* clone (GB: AA244730) was limited to whole kidney and uterus (73, 74). This enzyme showed strong activities catalyzing the sulfation of several prostaglandins, confirming the first association of eicosanoids with sulfotransferase activity in mammals (75). The positive role of eicosanoids in implantation events in the uterus has already been discussed (56).

This discussion has highlighted just a few examples of the differentially expressed endometrial genes within the epithelia and during implantation. We have not addressed whether the expression of these genes is regulated to the same extent at the translational level, because commercial availability of antibodies to relatively unknown genes is limited. However, we provide significant evidence that under receptive conditions, epithelial-specific genes of the mouse transcriptome can be dually or independently expressed in LE and GE populations. The molecular relationship between these epithelial subtypes is dynamic, the consequences of which are not fully understood, at least in terms of fertility. In future studies of the endometrium, it is imperative that their identity as specialized epithelial cell types be acknowledged, so that they are not studied as one type of epithelia but as separate entities.

Acknowledgments

We thank Ping Li for her outstanding technical assistance, Cheng Fan for SAM analysis, and Jim Lee for animal husbandry.

Received December 29, 2005. Accepted April 11, 2006.

Address all correspondence and requests for reprints to: Dr. Jeffrey W. Pollard, Department of Developmental and Molecular Biology, Albert Einstein College of Medicine, 1300 Morris Park Avenue, Bronx, New York 10461. E-mail: pollard@aecom.yu.edu.

Current address for A.L.N.: UCLA Department of Pathology, 650 Charles Young Drive, South, CHS 14-127, Los Angeles, California 90095.

This research was supported by grants from the National Institutes of Health (R01 CA 89617 to J.W.P.) and to the Albert Einstein Cancer Center (P30 13330). J.W.P. is the Sheldon and Betty E. Feinberg Senior Faculty Scholar in Cancer Research.

A.L.N. and J.W.P. have nothing to declare.

References

1. **Gray CA, Bartol FF, Tarleton BJ, Wiley AA, Johnson GA, Bazer FW, Spencer TE** 2001 Developmental biology of uterine glands. Biol Reprod 65:1311–1323
2. **Gray CA, Taylor KM, Ramsey WS, Hill JR, Bazer FW, Bartol FF, Spencer TE** 2001 Endometrial glands are required for preimplantation conceptus elongation and survival. Biol Reprod 64:1608–1613
3. **Fazleabas AT, Bazer FW, Roberts RM** 1982 Purification and properties of a progesterone-induced plasmin/trypsin inhibitor from uterine secretions of pigs and its immunocytochemical localization in the pregnant uterus. J Biol Chem 257:6886–6897
4. **Bell SC, Drife JO** 1989 Secretory proteins of the endometrium: potential markers for endometrial dysfunction. Baillieres Clin Obstet Gynaecol 3:271–291
5. **Dey SK, Lim H, Das SK, Reese J, Paria BC, Daikoku T, Wang H** 2004 Molecular cues to implantation. Endocr Rev 25:341–373
6. **Carson DD, Bagchi I, Dey SK, Enders AC, Fazleabas AT, Lessey BA, Yoshinaga K** 2000 Embryo implantation. Dev Biol 223:217–237
7. **Surveyor GA, Gendler SJ, Pemberton L, Das SK, Chakraborty I, Julian J, Pimental RA, Wegner CC, Dey SK, Carson DD** 1995 Expression and steroid hormonal control of Muc-1 in the mouse uterus. Endocrinology 136:3639–3647
8. **Stewart CL, Kaspar P, Brunet LJ, Bhatt H, Gadi I, Kontgen F, Abbondanzo SJ** 1992 Blastocyst implantation depends on maternal expression of leukaemia inhibitory factor. Nature 359:76–79
9. **Zhu LJ, Bagchi MK, Bagchi IC** 1998 Attenuation of calcitonin gene expression in pregnant rat uterus leads to a block in embryonic implantation. Endocrinology 139:330–339
10. **Miller C, Pavlova A, Sassoon DA** 1998 Differential expression patterns of Wnt genes in the murine female reproductive tract during development and the estrous cycle. Mech Dev 76:91–99
11. **Miller C, Sassoon DA** 1998 Wnt-7a maintains appropriate uterine patterning during the development of the mouse female reproductive tract. Development 125:3201–3211
12. **Parr BA, McMahon AP** 1995 Dorsalizing signal Wnt-7a required for normal polarity of D-V and A-P axes of mouse limb. Nature 374:350–353
13. **Niklaus AL, Babischkin JS, Aberdeen GW, Pepe GJ, Albrecht ED** 2002 Expression of vascular endothelial growth/permeability factor by endometrial glandular epithelial and stromal cells in baboons during the menstrual cycle and after ovariectomy. Endocrinology 143:4007–4017
14. **Rybicki AC, Fabry ME, Does MD, Kaul DK, Nagel RL** 2003 Differential gene expression in the kidney of sickle cell transgenic mice: upregulated genes. Blood Cells Mol Dis 31:370–380
15. **Tusher VG, Tibshirani R, Chu G** 2001 Significance analysis of microarrays applied to the ionizing radiation response. Proc Natl Acad Sci USA 98:5116–5121
16. **Livak KJ, Schmittgen TD** 2001 Analysis of relative gene expression data using real-time quantitative PCR and the $2^{-\Delta\Delta C}$T method. Methods 25:402–408
17. **Trogan E, Fisher EA** 2005 Laser capture microdissection for analysis of macrophage gene expression from atherosclerotic lesions. Methods Mol Biol 293:221–231
18. **Bi WL, Keller-McGandy C, Standaert DG, Augood SJ** 2002 Identification of nitric oxide synthase neurons for laser capture microdissection and mRNA quantification. Biotechniques 33:1274–1283
19. **Chen B, Zhang D, Pollard JW** 2003 Progesterone regulation of the mammalian ortholog of methylcitrate dehydratase (immune response gene 1) in the uterine epithelium during implantation through the protein kinase C pathway. Mol Endocrinol 17:2340–2354
20. **Luu KC, Nie GY, Salamonsen LA** 2004 Endometrial calbindins are critical for embryo implantation: evidence from in vivo use of morpholino antisense oligonucleotides. Proc Natl Acad Sci USA 101:8028–8033

21. **Paria BC, Das N, Das SK, Zhao X, Dileepan KN, Dey SK** 1998 Histidine decarboxylase gene in the mouse uterus is regulated by progesterone and correlates with uterine differentiation for blastocyst implantation. Endocrinology 139:3958–3966
22. **Cheng JG, Chen JR, Hernandez L, Alvord WG, Stewart CL** 2001 Dual control of LIF expression and LIF receptor function regulate Stat3 activation at the onset of uterine receptivity and embryo implantation. Proc Natl Acad Sci USA 98:8680–8685
23. **Stacey K, Beasley B, Wilce PA, Martin L** 1991 Effects of female sex hormones on lipid metabolism in the uterine epithelium of the mouse. Int J Biochem 23:371–376
24. **Hong SH, Nah HY, Lee JY, Lee YJ, Lee JW, Gye MC, Kim CH, Kang BM, Kim MK** 2004 Estrogen regulates the expression of the small proline-rich 2 gene family in the mouse uterus. Mol Cells 17:477–484
25. **Hewitt SC, Deroo BJ, Hansen K, Collins J, Grissom S, Afshari CA, Korach KS** 2003 Estrogen receptor-dependent genomic responses in the uterus mirror the biphasic physiological response to estrogen. Mol Endocrinol 17:2070–2083
26. **Tan YF, Li FX, Piao YS, Sun XY, Wang YL** 2003 Global gene profiling analysis of mouse uterus during the oestrous cycle. Reproduction 126:171–182
27. **Reese J, Das SK, Paria BC, Lim H, Song H, Matsumoto H, Knudtson KL, DuBois RN, Dey SK** 2001 Global gene expression analysis to identify molecular markers of uterine receptivity and embryo implantation. J Biol Chem 276:44137–44145
28. **Padilla L, Reinicke K, Montesino H, Villena F, Asencio H, Cruz M, Rudolph MI** 1990 Histamine content and mast cells distribution in mouse uterus: the effect of sexual hormones, gestation and labor. Cell Mol Biol 36:93–100
29. **Spaziani E** 1963 Relationship between early vascular responses and growth in the rat uterus: stimulation of cell division by estradiol and vasodilating amines. Endocrinology 72:180–191
30. **da Silva AJ, Li Z, de Vera C, Canto E, Findell P, Rudd CE** 1997 Cloning of a novel T-cell protein FYB that binds FYN and SH2-domain-containing leukocyte protein 76 and modulates interleukin 2 production. Proc Natl Acad Sci USA 94:7493–7498
31. **Langlois MR, Delanghe JR** 1996 Biological and clinical significance of haptoglobin polymorphism in humans. Clin Chem 42:1589–1600
32. **Carroll EA, Gerrelli D, Gasca S, Berg E, Beier DR, Copp AJ, Klingensmith J** 2003 Cordon-bleu is a conserved gene involved in neural tube formation. Dev Biol 262:16–31
33. **Sweadner KJ, Arystarkhova E, Donnet C, Wetzel RK** 2003 FXYD proteins as regulators of the Na,K-ATPase in the kidney. Ann NY Acad Sci 986:382–387
34. **Aizman R, Asher C, Fuzesi M, Latter H, Lonai P, Karlish SJ, Garty H** 2002 Generation and phenotypic analysis of CHIF knockout mice. Am J Physiol Renal Physiol 283:F569–F577
35. **Bernard O, Rachman F, Bennett D** 1981 Immunoglobulins in the mouse uterus before implantation. J Reprod Fertil 63:237–240
36. **Gobert AP, Cheng Y, Wang JY, Boucher JL, Iyer RK, Cederbaum SD, Casero Jr RA, Newton JC, Wilson KT** 2002 *Helicobacter pylori* induces macrophage apoptosis by activation of arginase II. J Immunol 168:4692–4700
37. **Watanabe H, Suzuki A, Mizutani T, Khono S, Lubahn DB, Handa H, Iguchi T** 2002 Genome-wide analysis of changes in early gene expression induced by oestrogen. Genes Cells 7:497–507
38. **Jeong JW, Lee KY, Kwak I, White LD, Hilsenbeck SG, Lydon JP, DeMayo FJ** 2005 Identification of murine uterine genes regulated in a ligand-dependent manner by the progesterone receptor. Endocrinology 146:3490–3505
39. **Yoshioka K, Matsuda F, Takakura K, Noda Y, Imakawa K, Sakai S** 2000 Determination of genes involved in the process of implantation: application of GeneChip to scan 6500 genes. Biochem Biophys Res Commun 272:531–538
40. **Hong SH, Nah HY, Lee JY, Gye MC, Kim CH, Kim MK** 2004 Analysis of estrogen-regulated genes in mouse uterus using cDNA microarray and laser capture microdissection. J Endocrinol 181:157–167
41. **Carson DD, Lagow E, Thathiah A, Al-Shami R, Farach-Carson MC, Vernon M, Yuan L, Fritz MA, Lessey B** 2002 Changes in gene expression during the early to mid-luteal (receptive phase) transition in human endometrium detected by high-density microarray screening. Mol Hum Reprod 8:871–879
42. **Borthwick JM, Charnock-Jones DS, Tom BD, Hull ML, Teirney R, Phillips SC, Smith SK** 2003 Determination of the transcript profile of human endometrium. Mol Hum Reprod 9:19–33
43. **Kao LC, Tulac S, Lobo S, Imani B, Yang JP, Germeyer A, Osteen K, Taylor RN, Lessey BA, Giudice LC** 2002 Global gene profiling in human endometrium during the window of implantation. Endocrinology 143:2119–2138
44. **Mirkin S, Arslan M, Churikov D, Corica A, Diaz JI, Williams S, Bocca S, Oehninger S** 2005 In search of candidate genes critically expressed in the human endometrium during the window of implantation. Hum Reprod 20: 2104–2117
45. **Takamoto N, Zhao B, Tsai SY, DeMayo FJ** 2002 Identification of Indian hedgehog as a progesterone-responsive gene in the murine uterus. Mol Endocrinol 16:2338–2348
46. **Suzuki N, Nadano D, Paria BC, Kupriyanov S, Sugihara K, Fukuda MN** 2000 Trophinin expression in the mouse uterus coincides with implantation and is hormonally regulated but not induced by implanting blastocysts. Endocrinology 141:4247–4254
47. **Murphy CR, Martin B** 1987 Digitonin cytochemistry reveals cholesterol-rich vesicles in uterine epithelial cells. Acta Histochem 81:143–147
48. **Murphy CR, Dwarte DM** 1987 Increase in cholesterol in the apical plasma membrane of uterine epithelial cells during early pregnancy in the rat. Acta Anat (Basel) 128:76–79
49. **Murphy DJ** 2001 The biogenesis and functions of lipid bodies in animals, plants and microorganisms. Prog Lipid Res 40:325–438
50. **Brasaemle DL, Barber T, Wolins NE, Serrero G, Blanchette-Mackie EJ, Londos C** 1997 Adipose differentiation-related protein is an ubiquitously expressed lipid storage droplet-associated protein. J Lipid Res 38:2249–2263
51. **Aoyama C, Liao H, Ishidate K** 2004 Structure and function of choline kinase isoforms in mammalian cells. Prog Lipid Res 43:266–281
52. **Weinhold PA, Rethy VB** 1974 The separation, purification, and characterization of ethanolamine kinase and choline kinase from rat liver. Biochemistry 13:5135–5141
53. **Malewicz B, Mukherjee JJ, Crilly KS, Baumann WJ, Kiss Z** 1998 Phosphorylation of ethanolamine, methylethanolamine, and dimethylethanolamine by overexpressed ethanolamine kinase in NIH 3T3 cells decreases the co-mitogenic effects of ethanolamines and promotes cell survival. Eur J Biochem 253:10–19
54. **Kiss Z** 1999 Regulation of mitogenesis by water-soluble phospholipid intermediates. Cell Signal 11:149–157
55. **Cheon YP, Xu X, Bagchi MK, Bagchi IC** 2003 Immune-responsive gene 1 is a novel target of progesterone receptor and plays a critical role during implantation in the mouse. Endocrinology 144:5623–5630
56. **Wang H, Dey SK** 2005 Lipid signaling in embryo implantation. Prostaglandins Other Lipid Mediat 77:84–102
57. **Pollard JW, Lin EY, Zhu L** 1998 Complexity in uterine macrophage responses to cytokines in mice. Biol Reprod 58:1469–1475
58. **Gouon-Evans V, Pollard JW** 2001 Eotaxin is required for eosinophil homing into the stroma of the pubertal and cycling uterus. Endocrinology 142:4515–4521
59. **Pollard JW** 1991 Lymphohematopoietic cytokines in the female reproductive tract. Curr Opin Immunol 3:772–777
60. **Robertson SA** 2000 Control of the immunological environment of the uterus. Rev Reprod 5:164–174
61. **Hunt JS, Petroff MG, Burnett TG** 2000 Uterine leukocytes: key players in pregnancy. Semin Cell Dev Biol 11:127–137
62. **King AE, Critchley HO, Kelly RW** 2003 Innate immune defences in the human endometrium. Reprod Biol Endocrinol 1:116
63. **Schalkwijk J, Wiedow O, Hirose S** 1999 The trappin gene family: proteins defined by an N-terminal transglutaminase substrate domain and a C-terminal four-disulphide core. Biochem J 340:569–577
64. **Hennighausen LG, Sippel AE** 1982 Characterization and cloning of the mRNAs specific for the lactating mouse mammary gland. Eur J Biochem 125:131–141
65. **Yanaihara A, Otsuka Y, Iwasaki S, Koide K, Aida T, Okai T** 2004 Comparison in gene expression of secretory human endometrium using laser microdissection. Reprod Biol Endocrinol 2:66
66. **Ace CI, Okulicz WC** 2004 Microarray profiling of progesterone-regulated endometrial genes during the rhesus monkey secretory phase. Reprod Biol Endocrinol 2:54
67. **Bowes D, Corrin B** 1977 Ultrastructural immunocytochemical localisation of lysozyme in human bronchial glands. Thorax 32:163–170
68. **Muller CA, Autenrieth IB, Peschel** 2005 Innate defenses of the intestinal epithelial barrier. Cell Mol Life Sci 62:1297–1307
69. **Cunliffe RN, Kamal M, Rose FR, James PD, Mahida YR** 2002 Expression of antimicrobial neutrophil defensins in epithelial cells of active inflammatory bowel disease mucosa. J Clin Pathol 55:298–304
70. **Hardman MJ, Sisi P, Banbury DN, Byrne C** 1998 Patterned acquisition of skin barrier function during development. Development 125:1541–1552
71. **Knight PA, Pemberton AD, Robertson KA, Roy DJ, Wright SH, Miller HR** 2004 Expression profiling reveals novel innate and inflammatory responses in the jejunal epithelial compartment during infection with *Trichinella spiralis*. Infect Immun 72:6076–6086
72. **Weinshilboum RM, Otterness DM, Aksoy IA, Wood TC, Her C, Raftogianis RB** 1997 Sulfation and sulfotransferases 1. Sulfotransferase molecular biology: cDNAs and genes. FASEB J 11:3–14
73. **Sakakibara Y, Yanagisawa K, Takami Y, Nakayama T, Suiko M, Liu MC** 1998 Molecular cloning, expression, and functional characterization of novel mouse sulfotransferases. Biochem Biophys Res Commun 247:681–686
74. **Shimada M, Terazawa R, Kamiyama Y, Honma W, Nagata K, Yamazoe Y** 2004 Unique properties of a renal sulfotransferase, St1d1, in dopamine metabolism. J Pharmacol Exp Ther 310:808–814
75. **Liu MC, Sakakibara Y, Liu CC** 1999 Bacterial expression, purification, and characterization of a novel mouse sulfotransferase that catalyzes the sulfation of eicosanoids. Biochem Biophys Res Commun 254:65–69

***Endocrinology* is published monthly by The Endocrine Society (http://www.endo-society.org), the foremost professional society serving the endocrine community.**